Seizure Detection of West Syndrome Based on Hybrid Optimization of Entropies With Multisensor EEG Data

Yue Bi, Duanpo Wu, Zhaoyang Xu, Pierre-Paul Vidal, Danping Wang, Yi Lin, Tiejia Jiang, Jiuwen Cao, *Senior Member, IEEE*, and Yuansheng Xu

***Abstract*—West syndrome is a persistent disease with a common, age-dependent, severe neurological disorder that poses a substantial risk to intellectual and motor deficits in children. Research on intelligent seizure detection methods for West syndrome can help doctors make effective judgments. In this article, we propose an infantile spasm seizure detection algorithm based on hybrid optimization of entropy of entropy (EoE) and Shannon entropy (SE). Different from traditional EoE and SE, fusion features are extracted from the optimal division of EoE (ODEoE) and optimal SE (OSE) by considering the epoch length and the number of subepochs in an epoch jointly. In addition, multivariate entropy parameterization via enhanced multistrategy sparrow algorithm (MEPEM-SSA) is employed for choosing the ideal parameters. Finally, the data from Zhejiang University School of Medicine Children's Hospital (ZUCH) dataset, the CHB-MIT dataset, and the Siena scalp electroencephalogram (EEG) dataset are extracted using EEG sensors, and a tenfold cross-validation evaluation is performed on these EEG data from West syndrome patients. The experimental results on the ZUCH dataset show that the mean values of precision, specificity, sensitivity, and *F*1 score of the algorithm are 98.08%, 97.93%, 98.46%, and 98.09% respectively. On the CHB-MIT dataset, the mean values of precision, specificity, sensitivity, and *F*1 score reach 98.76%, 99.27%, 97.94%, and 98.59%, respectively. On the Siena Scalp EEG dataset, the mean values of precision, specificity, sensitivity, and *F*1 score reach 98.33%, 98.04%, 98.39%, and 98.20%, respectively.**

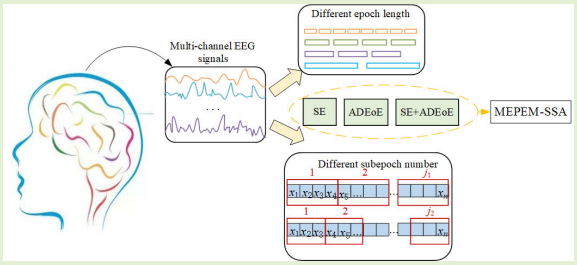

***Index Terms*— Electroencephalogram (EEG) sensor, entropy of entropy (EoE), seizure detection, Shannon entropy (SE), sparrow search algorithm (SSA).**

I. Introduction

WEST syndrome, one of the most prevalent age-dependent severe neurological illnesses, also known as infantile spasm, has a complicated cause and unknown mechanism [1]. The peak incidence of West syndrome is usually in infancy and early childhood [2]; 90% of patients experience their first syndrome symptom before the age of one year. The first spasmodic symptom of most kids appears within six months, and it typically affects children between the ages of three months and one year. Recurrent seizure can cause a variety of neurological conditions, including psychomotor abnormalities, developmental delays, and intellectual deficits [3], [4], [5]. The emergence of intelligent sensors has made remote detection of patient conditions relatively easy. These embedded sensors can detect different signals, such as electrocardiogram, electromyogram (EMG), and electroencephalogram (EEG). EEG signals contain a great deal of information about the functional behavior of the brain, and the most typical EEG waveforms are characterized by a significant number of sluggish, high-amplitude spikes that persist with a high level of randomness and disorder [6]. The experts detect the presence of seizure mainly on the EEG and clinical manifestations [7], [8], [9], which has

Manuscript received 29 March 2024; revised 15 August 2024; accepted 18 August 2024. Date of publication 27 August 2024; date of current version 16 October 2024. This work was supported in part by the National Natural Science Foundation of China under Grant 62301203, in part by the Graduate Scientific Research Foundation of Hangzhou Dianzi University under Grant CXJJ2023135, in part by the Fundamental Research Funds for the Provincial Universities of Zhejiang under Grant GK239909299001-401, in part by the National Key Research and Development Program under Grant 2021YFE0100100, in part by the Joint Fund of Zhejiang Provincial Natural Science Foundation of China under Grant LBY21H090001, and in part by NSFC-Zhejiang Integration Joint Fund under Grant U1909209. The associate editor coordinating the review of this article and approving it for publication was Prof. Octavian Postolache. *(Corresponding author: Duanpo Wu.)*

This work involved human subjects in its research. Approval of all ethical and experimental procedures and protocols was granted by the Ethic Committee of Zhejiang University under Application No. 2020-IRB-124.

Please see the Acknowledgment section of this article for the author affiliations.

Digital Object Identifier 10.1109/JSEN.2024.3447613

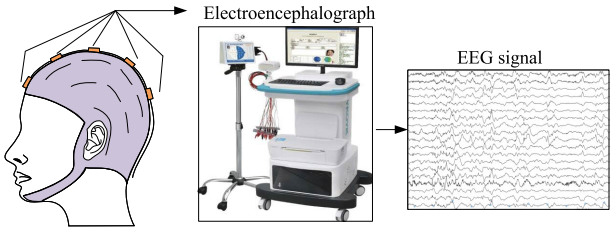

Fig. 1. EEG signal acquisition process.

problems such as biased judgment and is time-consuming. Accurately extracting hidden feature information from EEG signals has become a major challenge in biomedical signal processing [10], so it is necessary to introduce an efficient and intelligent algorithm for seizure detection [11], [12], [13].

Most traditional entropies can quantify a large amount of dynamic information about physiological signals obtained from sensors in a system. For example, the Kolmogorov–Sini entropy, which is the average rate of information generation or information dimension [14], [15], is a helpful parameter to characterize the dynamics of biological systems that take into consideration the correlation between various events, but it cannot be utilized to compute time series with finite length. Considering the insufficiency of Kolmogorov–Sini entropy, in order to calculate and analyze the characteristics of short time series more rationally, Pincus [16] proposed approximate entropy, which had been widely used in many fields such as physiology and medicine, but the final result had a large deviation. Shannon entropy (SE) estimates the uncertainty of the average information of all single occurrences, but it ignores the connections between them. These entropies are called single-scale entropies. Considering the shortcomings of single-scale entropies, Costa et al. [17] introduced the concept of time scale and subdivided the time series into windows of certain time scales for computation. They argued that the poor results of these entropies were related to their single-scale analysis method, which did not consider the complex fluctuations contained in the time series.

Hsu et al. [18] proposed an entropy of entropy (EoE) algorithm based on multiscale analysis. EoE combines multiscale entropy with the idea of kernel superinformation and calculates the quadratic entropy by slicing a time epoch into subepochs of a specific length that reflects the complexity of the time series and characterizes biological systems with information about changes hidden in the original time series. Inspired by EoE, Cui et al. [19] combined EoE with Deng entropy and proposed belief EoE (BEoE), which extended EoE to a confidence structure, and calculated the quadratic confidence entropy to characterize complex biological systems.

In the above papers, the EoE value is closely related to the number of subepochs and calculated by fixing the length of the epoch. However, the length of the epoch and the number of subepochs in an epoch have not been considered as important parameters for seizure detection. These parameters can be optimized by using the swarm intelligence algorithm.

In recent research, swarm intelligence algorithms have been used in a wide range of solving optimization problems. Yildirim et al. [20] searched for salient features for emotion recognition by using particle swarm optimization (PSO), cuckoo search (CS), gray wolf optimization (GWO), and dragonfly algorithm (DA). Lian et al. [21] proposed a new bionic whale optimization algorithm (WOA) to improve extremum values for EEG classification. Zhang et al. [22] used the artificial algorithm rabbit optimization (ARO) to select the optimal multibit local neighborhood difference pattern parameters (MLNDPs) for seizure detection. Attiya et al. [23] proposed a modified manta ray foraging optimization (MRFO) and salp swarm algorithm to handle the problem of scheduling tasks in cloud computing. Xue and Shen [24] proposed a sparrow search algorithm (SSA) in 2020, which is inspired by the search and counter-search behaviors of sparrows. SSA provides the benefits of a straightforward model, a minimal set of regulatory factors, and excellent decision accuracy compared to other animal search algorithms. However, SSA also suffers from defects such as insufficient convergence accuracy in the optimization process and is easy to fall into local optimal solutions in complex cases, which requires further research and optimization. Many researchers have improved SSA to address its deficiencies. Yuan et al. [25] used the center of gravity reverse learning mechanism and variation operator to improve the SSA algorithm so that it avoids falling into the local extremes. Gao et al. [26] combined SSA with a greedy strategy to make full use of all the individuals in the sparrow population and improved the search accuracy. The above algorithms increase the algorithm's ability to find the optimal to a certain extent, but SSA needs to be improved in terms of search range and search accuracy. On the basis of SSA, this article proposes a multivariate entropy parameterization via enhanced multistrategy SSA (MEPEM-SSA) by adding tent chaotic mapping and a random walk strategy. It is mainly improved by two parts: 1) before the sparrow search, using

TABLE I
DETAILS OF THE ZUCH DATASET

ID	Gender	Age	Seizure time (s)	Seizure number
IS_1	M	1y	263	1
IS_2	F	1y	278	1
IS_3	M	6m16d	874	2
IS_4	M	6m23d	306	1
IS_5	M	7m10d	203	1
IS_6	M	4m17d	274	1
IS_7	M	9m12d	345	1
IS_8	F	4m9d	336	2
IS_9	M	5m4d	752	2
IS_10	F	6m25d	203	1
IS_11	F	1y6m	387	2
IS_12	F	6m25d	259	1
IS_13	M	4m9d	639	1
IS_14	M	7m24d	98	1
IS_15	M	7m23d	142	1
IS_16	M	1y	173	1
IS_17	M	6m7d	434	1
IS_18	M	1y5m	318	1
IS_19	M	4m28d	137	2
IS_20	F	4m18d	175	1
IS_21	M	2m19d	110	1
IS_22	M	6m4d	958	2
IS_23	F	4m15d	132	1
IS_24	F	11m16d	511	1
IS_25	M	7m24d	228	1

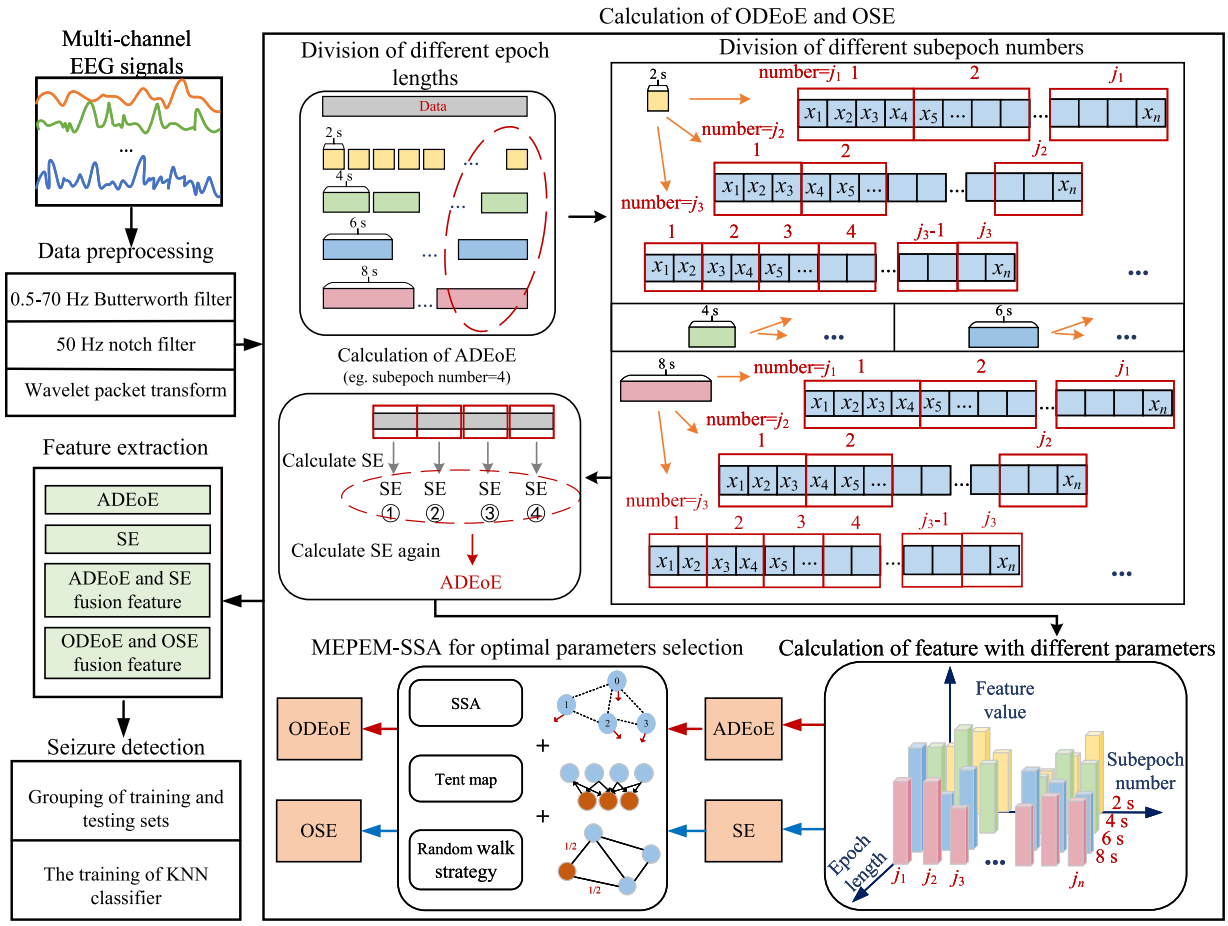

Fig. 2. Framework for categorizing EEG signals in West syndrome.

tent chaotic mapping to increase the randomness of the initial population, so as to make its individual coverage wider and increase the diversity of the search and 2) after the sparrow search, adding the random walk strategy to optimize the sparrow's position for further updating, so as to avoid the algorithm falling into the local optimum.

This article studies the variability of the optimal division of EoE (ODEoE) parameters by extracting EEG signals from sensors, using both epoch length and the number of subepochs as adjustable parameters for ODEoE. Then ODEoE is fused with optimal SE (OSE) as features for classification, and the use of the MEPEM-SSA algorithm is proposed for parameter optimization. The algorithm is ultimately combined with an EEG diagnostic instrument for seizure detection. The rest of the article is presented as follows. Section II describes the data preprocessing, calculation of ODEoE and OSE, MEPEM-SSA, and feature extraction work. Section III analyzes the results. Sections IV and V discuss and conclude this article.

II. Dataset and Methodology

The method first preprocesses the data, performs wavelet packet transform (WPT) of the preprocessed multichannel EEG signal, calculates ODEoE with the obtained wavelet packet coefficients, then selects the optimal epoch length using the improved SSA algorithm, and, finally, inputs the feature into three classifiers for West syndrome classification. The EEG signal acquisition process and classification scheme for West syndrome EEG signals are shown in Figs. 1 and 2, respectively, and each step's specifics will be described as follows.

A. Dataset Description

The experiments are conducted on three epilepsy datasets extracted by multichannel sensors: the CHB-MIT dataset [27], the Siena Scalp EEG dataset, and the Zhejiang University School of Medicine Children's Hospital (ZUCH) dataset.

1) The CHB-MIT dataset was collected at Children's Hospital Boston. There are a total of 24 records in the dataset (case 24 subject is unknown), and the remaining 23 records are from 22 subjects. The CHB-MIT dataset has a sampling rate of 256 Hz and typically contains 23 channels of EEG signals [28]. In all, 181 seizure fragments are used in this article, lasting for 6 h. The epileptic seizures last for approximately 3 h, and the seizure-free period lasts for approximately 3 h.

2) The Siena Scalp EEG dataset [29] contains EEG recordings from 14 patients with 29 channels obtained from the University of Siena. The subjects include nine men (25–71 years) and five women (20–58 years). The sampling rate of this dataset is 512 Hz.

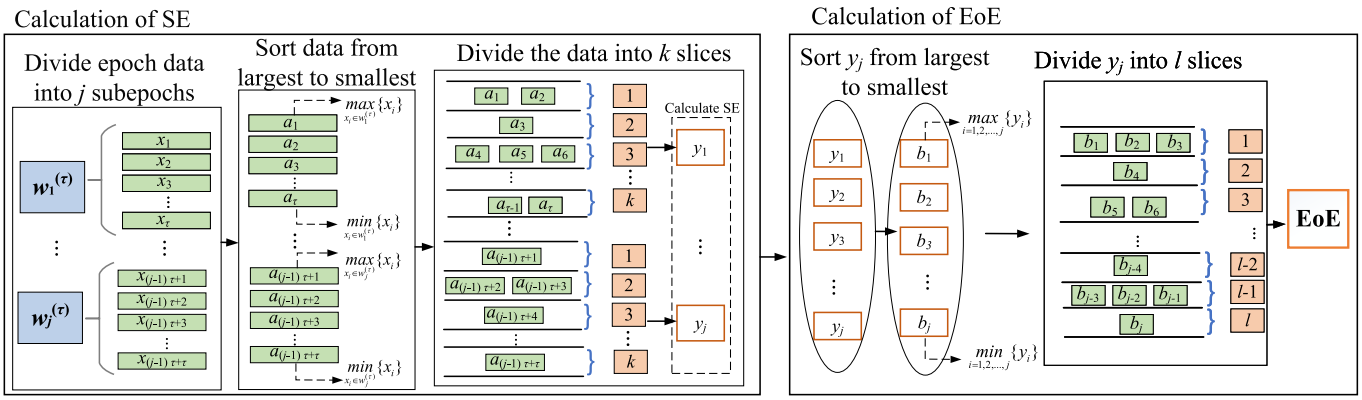

Fig. 3. Flowchart of EoE calculation.

3) The long-term EEG data of 25 West syndrome patients (IS_1 to IS_25) were gathered from the ZUCH, including 21 channels with a sampling rate of 1000 Hz. Detailed information about the patient's gender, age, and pathology for each scalp EEG can be seen in Table I.

International 10–20 electrode placement system [30] was used to record EEG signals.

B. Data Preprocessing

1) Butterworth Filter and Notch Filter: The raw EEG signals are interfered with external noise and the patient's body movement during the acquisition process. Considering the interference of eye movements on the signals, the channel data related to Fp1 and Fp2 are removed, and finally, 20 bipolar (BP) lead channel data can be obtained on these datasets, which are "F7-T3," "T3-T5," "T5-O1," "F8-T4," "T4-T6," "T6-O2," "F3-C3," "C3-P3," "P3-O1," "F4-C4," "C4-P4," "P4-O2," "FZ-CZ," "CZ-PZ," "F7-F3," "T3-C3," "T5-P3," "F4-F8," "C4-T4," and "P4-T6."

In addition, to minimize the effect of high-frequency noise, a 0.5–70-Hz Butterworth filter and a 50-Hz notch filter are used to filter out the industrial interference and eliminate interference from extremely high and extremely low frequencies. Finally, the preprocessing of multichannel sensor EEG signals is completed.

2) WPT: WPT can also be called wavelet packet or subband tree and optimal subband tree structuring. The idea is to use the analysis tree to represent the wavelet packet or employ various superpositions of wavelet transformations to study the specifics of the input signal. It divides the frequency band into multiple levels, decomposes the signal into wavelets with different frequencies, and further decomposes the high-frequency part that is not subdivided by the multiresolution analysis. It can also adaptively select the corresponding frequency band according to the characteristics of the signal being analyzed to match the signal spectrum to improve the time–frequency resolution. Different from discrete wavelet transform (DWT), WPT binarizes the division of high- and low-frequency bands and obtains the approximation coefficients through layer-by-layer decomposition at the same time, and finally, the whole band is divided into uniform subbands; the final decomposed multifrequency bands can be described as a tree-like structure known as wavelet packet tree.

This article combines the EoE algorithm with WPT, and DB4 is selected as the wavelet gene because it can effectively extract the frequency characteristics of signals and suppress noise. In WPT, the more decomposition levels there are, the easier it is to lose signal details. However, if the decomposition level is too low, noise cannot be removed. In this experiment, we select the frequency band of 0.5–125 Hz for analysis to reflect the changes of hidden information in different frequency bands, which is very helpful for subsequent feature processing and classification performance. Because the three EEG sensor datasets that we use have different sampling frequencies, in order to ensure consistency in the frequency of wavelet packet nodes on them, a three-layer WPT is used on the CHB-MIT dataset, a four-layer WPT is used on the Siena Scalp EEG dataset, and a five-layer WPT is used on the ZUCH dataset. Finally, select the wavelet packet coefficients of the first eight nodes in the last layer to cover the frequency range of 0.5–125 Hz.

C. Calculation of ODEoE and OSE

1) Steps of the EoE Method: The methodology for EoE analysis consists of two steps. First, SE is used to characterize the state of the system over a time window, representing the information contained in that time period. Second, SE is also used to characterize the uncertainty of information states. The flowchart of the computation is shown in Fig. 3.

Step 1: First, the original time series is denoted as $\{x_i\}$, and the multidimensional discrete time series of length n is divided into consecutive nonoverlapping subepochs $\{w_j^{(\tau)}\}$. Each subepoch $w_j^{(\tau)}$ is of length τ, where $w_j^{(\tau)} = \{x_{(j-1)\tau+1}, x_{(j-1)\tau+2}, \ldots, x_{(j-1)\tau+\tau}\}$, and j is the subepoch index from 1 to $\lfloor n/\tau \rfloor$. We denote the original time series as $\{x_i\}$ and sort $\{x_i\}$ from largest to smallest, which can be represented as $\{a_i\}$.

Then, separate $\{a_i\}$ into s_1 slices, $s_1 \in [x_{\min}, x_{\max}]$, so that each slice corresponds to a distinct physiological state. The following equation can be used to determine the probability p_{jk} that a particular interval x_i on a subepoch $w_j^{(\tau)}$(τ is the

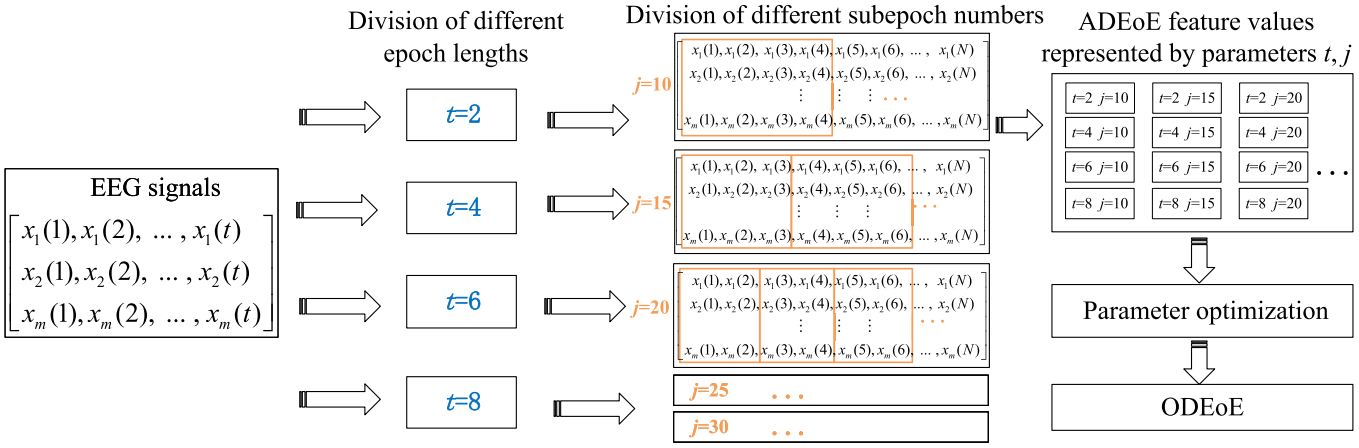

Fig. 4. Flowchart of ODEoE calculation.

series length of a subepoch) exists in state k

$$p_{jk} = \frac{\text{total number of } x_i \text{ over } w_j^{(\tau)} \text{ in state } k}{\tau} \tag{1}$$

where k is the state index from 1 to s_1. The SE value $y_j^{(\tau)}$ of each subepoch $w_j^{(\tau)}$ can be calculated by the following equation:

$$y_j^{(\tau)} = -\sum_{k=1}^{s_1} p_{jk} \ln p_{jk}. \tag{2}$$

Step 2: SE is used again to measure the degree of information change in $y_j^{(\tau)}$. l is the index of the interval from 1 to s_2, $s_2 \in [y_{\min}, y_{\max}]$. The sorted list of $y_j^{(\tau)}$ from largest to smallest is represented as $\{b_i\}$ $(i \in [1, j])$ in Fig. 3. The following equation can be used to determine the probability p_l that $y_j^{(\tau)}$ exists in state l:

$$p_l = \frac{\text{total number of } y_j^{(\tau)} \text{ over } \left\{y_j^{(\tau)}\right\} \text{ in state } l}{n/\tau}. \tag{3}$$

Therefore, the SE value of the sequence $y_j^{(\tau)}$, which is also the EoE value of series $\{x_i\}$, is given by the following equation:

$$\text{EoE} = -\sum_{l=1}^{s_2} p_l \ln p_l. \tag{4}$$

2) Steps of the ODEoE Method: Based on the EoE algorithm, this article considers the length of the epoch and the number of subepochs to be adjustable parameters. The adjustable division of EoE (ADEoE) is calculated by changing these two parameters at the same time. ODEoE is the optimal value after parameter optimization for ADEoE, and the block diagram of ODEoE calculation is shown in Fig. 4.

First, the original multichannel EEG signals are sliced into four sets of data segments with lengths of epochs, which can be represented as t, and its unit is seconds. Next, the number of subepochs is represented as j, $j \in [5, 30]$. If j is selected to be too large or too small, it will result in insufficient data points to fully represent the degree of information change in each epoch when calculating the second SE. When the first step of the ODEoE algorithm is performed, the SE value of each subepoch will be computed for each group of data with a different parameter j, and the probability can be calculated by the following equation:

$$p_{jk} = \frac{\text{total number of } x_i \text{ over } w_j^{(\tau)} \text{ in state } k}{\tau}, \quad j \in [5, 30]. \tag{5}$$

Then, the SE is calculated again by (6), and the ADEoE value of the original time series $\{x_i\}$ is calculated and is given by the following equation:

$$p_l(t, j) = \frac{\text{total number of } y_j^{(\tau)} \text{ over } \left\{y_j^{(\tau)}\right\} \text{ in state } l}{t/\tau} \tag{6}$$

$$\text{ADEoE}(t, j) = -\sum_{l=1}^{s_2} p_l(t, j) \ln p_l(t, j). \tag{7}$$

After that, ADEoE that can be indexed by t and j can be obtained, for example, $(t = 2, j = 10)$ is denoted as the range of ADEoE value when the epoch length is 2 and the number of subepochs is 10.

Then, we use R_{ac} to evaluate the performance of different parameters, which can be obtained by the following equation:

$$R_{\text{ac}}(t, j) = \frac{\sum_{a=1}^{N_s} Q(t, j)}{N_s} \tag{8}$$

where N_s is the actual number of seizures and $Q(t, j)$ is the number of seizures obtained by using ADEoE.

Finally, we optimize the algorithm to find the optimal parameters for ADEoE, denoted by t^* and j^*, which are the indexes where accuracy is the highest value among all ADEoE values and record the ADEoE at this time as ODEoE. The calculation formulas are given as follows:

$$\left\{t^*, j^*\right\} = \underset{t^* \in A, j^* \in B}{\text{argmax}} \left\{R_{\text{ac}}(\text{ADEoE}(t, j))\right\} \tag{9}$$

$$\text{ODEoE} = \text{ADEoE}\left(t^*, j^*\right) \tag{10}$$

where $A \in [2, 8]$ and $B \in [5, 30]$.

3) Steps of the OSE Method: First, the data with epoch length t were recorded as $\{x_t\}$ and separated into s_3 slices, $s_3 \in [x_{\min}, x_{\max}]$, so that each slice corresponds to a distinct physiological state. The following equation can be used to determine the probability p_b that a particular interval x_t exists in state b:

$$p_b(t) = \frac{\text{total number of } x_t \text{ in state } b}{t} \tag{11}$$

where b is the state index from 1 to s_3. The SE value can be calculated by the following equation:

$$\mathrm{SE}(t) = -\sum_{b=1}^{s_3} p_b(t) \ln p_b(t). \tag{12}$$

Then, we optimize the algorithm to find the optimal parameters for SE and record SE at this time as OSE. R_{ac} is used to evaluate the performance of different parameters. The calculation formulas are given as follows:

$$R_{\mathrm{ac}}(t) = \frac{\sum_{a=1}^{N_s} Q(t)}{N_s} \tag{13}$$

$$\{t^*\} = \underset{t^* \in A}{\operatorname{argmax}} \{R_{\mathrm{ac}}(\mathrm{SE}(t))\} \tag{14}$$

$$\mathrm{OSE} = \mathrm{SE}(t^*) \tag{15}$$

where $Q(t)$ is the number of seizures obtained by using SE.

D. Feature Extraction

In this study, we meticulously leverage SE, ADEoE, ADEoE + SE fusion feature, and ODEoE + OSE fusion feature extracted from each of the 20 channels of EEG sensor data. Employing a systematic approach, each channel undergoes a comprehensive decomposition through WPT, from which the initial eight nodes are extracted, resulting in a total of 160 subbands. For each subband, a distinct feature is meticulously computed. Our analysis focuses on the derivation of four distinct features essential for West syndrome seizure detection:

1) SE as the feature;
2) ADEoE as the feature;
3) ADEoE + SE fusion feature;
4) ODEoE + OSE fusion feature.

E. MEPEM-SSA for Optimal ODEoE + OSE Fusion Feature Parameters Selection

This section introduces the MEPEM-SSA, a novel approach for the selection of optimal parameters in ODEoE + OSE fusion feature optimization. MEPEM-SSA builds upon the conventional SSA by incorporating multiple strategies to overcome intrinsic limitations. Functioning as a recently devised intelligent optimization algorithm, SSA intricately replicates the search dynamics exhibited by a sparrow flock, offering rapid solution speed and high accuracy. However, despite its merits, SSA is not without limitations. This section systematically addresses these drawbacks, employing a diverse array of strategies to enhance the MEPEM-SSA algorithm specifically for the parameter optimization of ODEoE + OSE fusion features. Fig. 5 shows the flowchart for selecting the optimal

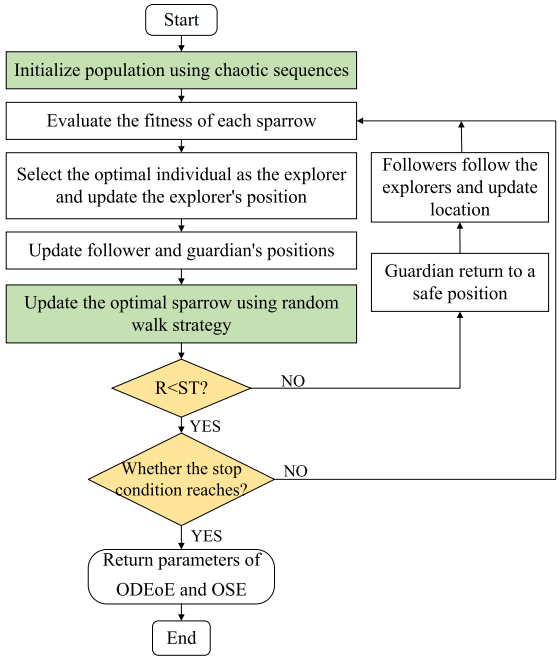

Fig. 5. Flowchart of ODEoE + OSE fusion feature parameter optimization selection.

TABLE II
MEPEM-SSA PARAMETER SETTINGS

Parameter	Value
ST	0.6
PD	0.7
SD	0.2
Number of sparrows in the population	10
Maximum number of iterations	5

ODEoE and OSE parameters, and Table II shows the detailed parameter settings of MEPEM-SSA. Among them, ST is the warning value, PD is the ratio of discoverers, and SD is the followers.

1) Tent Chaos Mapping: To address the stochastic variability inherent in SSA's initial population, MEPEM-SSA introduces tent chaos mapping. This strategic integration ensures a more uniform distribution of initial solutions across the solution space. Unlike the random generation of the initial SSA population, the incorporation of tent chaotic mapping enhances the diversity and coverage of the population, promoting improved global optimization performance in later algorithmic stages. The position of the ith sparrow in the kth iteration can be expressed as

$$x_i^k = \left(T_i^k, J_i^k\right) \tag{16}$$

where T_i^k and J_i^k are the length of epoch and the number of subepochs of the ith ADEoE + SE fusion feature in the kth iteration, respectively. $i \in [1, N], k \in [1, k_{\max}]$. N and $k_{\max}$ are the number and maximum number of iterations of sparrows, respectively.

The expression for generating chaotic sequences based on tent mapping is shown in the following equation:

$$z_{i+1}^k = \begin{cases} \dfrac{z_i^k}{u}, & 0 \le z_i^k \le u \\ \dfrac{1 - z_i^k}{1 - u}, & u < z_i^k \le 1 \end{cases} \tag{17}$$

where $u \in \text{rand}(0, 1)$, the chaotic sequence generated by (17) is introduced into the space to be solved, and a sequence of the initial positions of individual sparrows in the search region is further generated, as shown in the following equation:

$$x_i^k = x_{i,\min}^k + z_i^k \left(x_{i,\max}^k - x_{i,\min}^k \right) \tag{18}$$

where $x_{i,\max}^k$ and $x_{i,\min}^k$ denote the maximum and minimum values of the sequence, respectively. Then, the position of each sparrow is applied to the ODEoE + OSE fusion feature code, and the fitness value of each sparrow is calculated to evaluate the performance of the ODEoE + OSE fusion feature.

2) Random Walk Strategy: Addressing SSA's propensity for local optima entrapment, MEPEM-SSA employs a random walk strategy. The random walk strategy is a mathematical, statistical model that cannot represent the motion trajectory generated by any regular motion [31]. The random walk process can be expressed as follows. Equations (19) and (20) delineate the process of dynamically updating ODEoE and OSE parameters, significantly augmenting the local search efficiency and facilitating the identification of optimal epoch lengths and subepoch numbers for the fusion feature algorithm

$$X(k) = \{0, c_u (2r(k_1) - 1), \ldots, c_u (2r(k_n) - 1)\} \tag{19}$$

where $X(k)$ is the set of randomized wandering steps, c_u is the cumulative sum of wandering steps, k_n is the number of steps of the nth randomized wandering, and $r(k)$ is the expression of the random function.

The process of updating ODEoE and OSE parameters can be expressed, as shown in the following equation:

$$x_i^k = \frac{\left(x_i^k - a_i\right)\left(d_i^k - c_i^k\right)}{(b_i - a_i)} + c_i^k \tag{20}$$

where x_i^k denotes the position of the ith sparrow in the kth iteration, a_i and b_i are the minimum and maximum values of the i-dimensional variables, and c_i^k and d_i^k are the minimum and maximum values of the i-dimensional variables in the kth iteration. The random walk strategy is helpful to improve the efficiency of the local search for the best position and find the optimal epoch length and number of subepochs for the ODEoE + OSE fusion feature algorithm.

Through the application of MEPEM-SSA, the parameter selection process for ODEoE + OSE fusion features is not only optimized but also elevated to a higher echelon of precision and efficiency. This novel approach, grounded in the principles of stratified optimization and enhanced multi-strategy, heralds a new era in the field of biomedical signal processing, particularly in the detection of infantile spasm seizures.

TABLE III
CHANGES IN CLASSIFICATION PERFORMANCE OF ADEoE DUE TO DIFFERENT t'S WHEN $j = 20$ ON THE ZUCH DATASET

	Classifier	t=1(%)	t=2(%)	t=3(%)	t=4(%)	t=5(%)	t=6(%)	t=7(%)	t=8(%)
ACC	RF	88.49	88.47	89.06	88.98	89.05	89.43	89.46	89.38
	KNN	96.16	96.11	96.46	96.27	96.40	97.36	96.80	96.98
	SVM	92.11	91.39	92.43	91.25	91.04	91.21	91.26	91.95
PRE	RF	87.18	86.85	87.04	86.30	86.60	86.74	87.19	86.54
	KNN	96.54	96.55	96.41	96.69	95.97	97.19	96.70	96.66
	SVM	91.78	90.84	91.64	89.78	89.14	88.90	88.76	89.36
SEN	RF	90.26	90.67	91.81	92.71	92.41	93.14	92.46	93.34
	KNN	95.76	95.64	96.49	95.83	96.89	97.54	96.93	97.35
	SVM	92.50	92.09	93.42	93.12	93.44	94.18	94.48	95.27
F1	RF	88.69	88.71	89.34	89.38	89.39	89.82	89.74	89.79
	KNN	96.15	96.09	96.45	96.26	96.42	97.36	96.81	96.99
	SVM	92.14	91.45	92.50	91.41	91.23	91.46	91.52	92.21

3) Time Complexity Analysis of MEPEM-SSA: Time complexity analysis typically relies on three rules: population initialization, computing fitness functions, and updating solutions. Assuming that the population size is N, T is the total number of iterations, and D is the spatial dimension of the solution. $O(N)$ is the computational complexity of the population initialization process, and the time complexity of calculating fitness is $O(D)$. The computational complexity of the solution update process is $O(\text{TN}) + O(\text{TND})$. MEPEM-SSA has added tent chaos mapping and random walk strategy, both of which have a computational complexity of $O(\text{TN})$. Therefore, the overall time complexity of the MEPEM-SSA algorithm is $O(NT) + O(T)[O(N^2) + O(D)] = O(\text{TN}^2)$.

III. EXPERIMENTAL RESULTS

In this section, a series of experiments are performed on three datasets. These datasets include two public datasets and one dataset from ZUCH, and training data together with these datasets can determine whether the method has universality and transferability through analysis conclusions. First, we examine the effect of the parameters in ADEoE on the performance. Second, we apply three feature values of ADEoE, SE, and ADEoE fused with SE to datasets, and to analyze the performance of three different models in detecting seizure in West syndrome, classification results are obtained. Then, the feature values fused with ODEoE and OSE will be optimized for parameters in SSA, ARO, GWO, and MEPEM-SSA, and their performance will be compared. Finally, the results of different methods in seizure detection will be analyzed.

A. Performance Indicators

In this article, 90% of the EEG sensor data are divided into a training set, and the remaining 10% are used as a validation set, using random forest (RF), K-nearest neighbor (KNN), and support vector machine (SVM) classifiers to classify epileptic seizures. The confusion matrix is calculated by tenfold cross-validation to show the classification performance of this

TABLE IV
CHANGES IN CLASSIFICATION PERFORMANCE OF ADEOE DUE TO DIFFERENT j'S WHEN $t = 6$ ON THE ZUCH DATASET

	Classifier	j=5(%)	j=10(%)	j=15(%)	j=20(%)	j=25(%)	j=30(%)
ACC	RF	82.73	87.20	86.87	89.43	89.27	91.10
	KNN	88.15	96.21	94.91	97.36	96.34	96.87
	SVM	84.85	89.60	89.98	91.21	91.76	92.29
PRE	RF	79.37	84.19	84.28	86.74	87.26	89.22
	KNN	83.95	94.87	94.04	97.19	95.91	96.59
	SVM	82.24	94.87	87.98	88.90	89.92	90.93
SEN	RF	88.50	91.68	90.69	93.14	92.02	93.57
	KNN	94.40	97.71	95.92	97.54	96.84	97.20
	SVM	88.97	93.48	92.65	94.18	94.10	93.97
F1	RF	83.67	87.76	87.35	89.82	89.56	91.33
	KNN	88.84	96.27	94.96	97.36	96.36	96.88
	SVM	85.44	89.99	90.23	91.46	91.95	92.41

algorithm, and the number of true positive, true negative, false positive, and false negative can be represented as TP, TN, FP, and FN, respectively. Based on the above indicators, accuracy, specificity, sensitivity, and $F1$ scores can be calculated as ACC, PR, SEN, and $F1$, respectively. The formulas are given as follows:

$$\mathrm{ACC} = \frac{\mathrm{TP} + \mathrm{TN}}{\mathrm{TP} + \mathrm{FP} + \mathrm{TN} + \mathrm{FN}} \tag{21}$$

$$\mathrm{PRE} = \frac{\mathrm{TP}}{\mathrm{TP} + \mathrm{FP}} \tag{22}$$

$$\mathrm{SEN} = \frac{\mathrm{TP}}{\mathrm{TP} + \mathrm{FN}} \tag{23}$$

$$F1 = \frac{2\mathrm{TP} \times \mathrm{SEN}}{\mathrm{TP} + \mathrm{SEN}\,(\mathrm{TP} + \mathrm{FP})} \tag{24}$$

B. ZUCH Dataset Result

In the calculation process, different values of parameters t and j can lead to different ADEoE values, resulting in different accuracy of classification.

In Table III, this article first compares the classification performance differences of RF, KNN, and SVM classifiers with different t values when $j = 20$. From the conclusion, it can be seen that using different classifiers has a significant impact on the experimental indicators. When $t = 1$, the difference in ACC reaches 7.67% when using KNN and RF, respectively. RF has the worst classification performance among the three classifiers, followed by SVM, while KNN has the best classification performance. It can also be seen that when $j = 20$, there is a significant difference in the classification performance of epileptic seizure detection by changing the t value. After calculating ADEoE at different t's, it is found that all four performance indicators show an overall trend of first increasing and then decreasing. When $t = 6$, there are the highest ACC, PRE, SEN, and $F1$ values when using KNN, which are 97.36%, 97.19%, 97.54%, and 97.36%, respectively. Table IV compares the classification performance differences of RF, KNN, and SVM classifiers with different j values when $t = 6$. The classification performance of KNN is still superior to other classifiers. The classification results change with the change of parameter j. When $j = 20$, ACC, PRE, and $F1$ reach their maximum values on KNN at 97.36%, 97.19%, and 97.36%, respectively. When $j = 10$, SEN has a maximum value of 97.71% on KNN. Combining these two conclusion tables, it can be concluded that the changes in parameters t and j have a great influence on the final classification results. Both of them are important adjustable parameters of ADEoE, and by simultaneously optimizing t and j, the optimal ADEoE for classification results can be found. Finally, through experiments, it is found that when $t = 6$ and $j = 20$, KNN performs the best, with ACC reaching 97.36%. The optimal parameters of ADEoE will be applied to subsequent calculations.

Next, three different feature values are used as the computational model for seizure detection. To determine the effectiveness of this method, we investigate the performance of ADEoE, SE, and ADEoE + SE fusion features. Table V shows the classification performance on 25 patients when using different feature values on KNN. From the results, it can be concluded that ADEoE is generally better than SE. Comparing the three feature values based on the average classification results of all patients, the ACC, PRE, SEN, and $F1$ of ADEoE + SE fusion features are higher than those of performances using SE and ADEoE alone.

Then, the optimal parameter j is kept unchanged, and we use SSA, ARO, and GWO combined with MEPEM-SSA, respectively, to perform optimization analysis on the parameter t in the ADEoE + SE fusion feature. At this point, the features are represented as ODEoE + OSE fusion features. As demonstrated in Table V, MEPEM-SSA combined with ODEoE + OSE fusion feature yields the highest ACC values in all patients. However, for $F1$, PRE, and SEN metrics, MEPEM-SSA combined with ODEoE + OSE fusion feature does not reach the best classification ACC. For IS_1, $F1$ of ADEoE reaches the maximum value of 99.23% when $t = 6$ and $j = 20$; for IS_8, SEN of ADEoE + SE fusion feature reaches the maximum value of 100% when $t = 6$, and SEN of ARO and GWO combined with OSE + ODEoE also reach the maximum value of 100%; for IS_10, PRE of ARO combined with OSE + ODEoE reaches the maximum value of 99.43%; for IS_11, PRE of GWO combined with OSE + ODEoE reaches the maximum value of 100%; for IS_15, PRE of SE reaches the maximum value of 100% when $t = 8$, and ARO and GWO combined with OSE + ODEoE reach the maximum value of 100%; for IS_20, PRE of ADEoE, SE, ADEoE + SE fusion feature, ARO, and GWO combined with OSE + ODEoE reach the maximum value of 100%; for IS_22, PRE of GWO combined with OSE + ODEoE reaches the maximum value of 98.50%, and $F1$ of GWO combined with OSE + ODEoE reaches the maximum value of 99.22%; and for IS_23, SEN reaches the maximum value of 100% when SSA, ARO, and GWO are used. However, for the average of 25 patients, the method of MEPEM-SSA combined with ODEoE + OSE fusion feature yields the best results of classification, with average ACC, PRE, SEN, and $F1$ metrics of 98.08%, 97.93%, 98.46%, and 98.09%, respectively.

TABLE V
SUBJECT COMPARISON OF DIFFERENT METHODS ON THE ZUCH DATASET

	ADEoE	SE				SE+ADEoE				OSE+ODEoE			
		t=2	t=4	t=6	t=8	t=2	t=4	t=6	t=8	SSA	ARO	GWO	MEPEM-SSA
	IS_1												
ACC	99.11%	96.15%	96.92%	97.65%	97.50%	96.73%	97.69%	98.24%	97.50%	98.50%	98.34%	98.57%	**99.29%**
PRE	100%	100%	100%	100%	100%	100%	100%	100%	100%	100%	100%	93.33%	**100%**
SEN	98.57%	92.05%	93.87%	95.60%	95.65%	93.42%	95.21%	96.32%	95.65%	96.69%	94.15%	97.64%	**97.33%**
F1	**99.23%**	95.82%	96.78%	97.66%	97.66%	96.58%	97.48%	98.04%	97.66%	98.24%	98.40%	98.75%	98.56%
	IS_2												
ACC	99.23%	99.64%	99.26%	100%	100%	99.64%	99.26%	100%	100%	100%	100%	100%	**100%**
PRE	100%	99.67%	100%	100%	100%	99.67%	100%	100%	100%	100%	100%	100%	**100%**
SEN	98.75%	99.67%	98.54%	100%	100%	99.67%	98.54%	100%	100%	100%	100%	100%	**100%**
F1	99.33%	99.67%	99.24%	100%	100%	99.67%	99.24%	100%	100%	100%	100%	100%	**100%**
ACC	98.52%	98.80%	98.89%	98.89%	100%	98.52%	98.52%	99.17%	99.63%	99.63%	99.33%	99.19%	**99.72%**
PRE	99.38%	98.32%	98.23%	97.87%	100%	97.78%	97.53%	98.29%	99.44%	99.38%	98.64%	98.39%	**99.51%**
SEN	97.91%	99.28%	99.64%	100%	100%	99.25%	99.64%	100%	100%	100%	100%	100%	**100%**
F1	98.59%	98.78%	98.92%	98.91%	100%	98.50%	98.56%	99.12%	99.71%	99.68%	99%	99.17%	**100%**
	IS_4												
ACC	99.06%	99.23%	98.75%	98.10%	98.13%	99.08%	99.06%	98.57%	98.13%	98.25%	99.22%	99.06%	**99.26%**
PRE	98.24%	98.81%	97.68%	97.27%	97.50%	98.44%	98.20%	97.31%	96.39%	98.20%	98.54%	98.33%	**98.59%**
SEN	100.00%	99.71%	100%	99.29%	99.00%	99.705	100%	100%	100%	100%	100%	100%	**100%**
F1	99.07%	99.24%	98.79%	98.22%	98.05%	99.055	99.07%	98.59%	97.98%	99.01%	99.25%	99.13%	**99.27%**
	IS_5												
ACC	96.00%	96.23%	96.33%	96.50%	96.67%	96.07%	96.33%	96.00%	96.67%	97.37%	96.74%	97.04%	**97.73%**
PRE	93.73%	94.52%	94.25%	93.86%	94.49%	94.00%	93.39%	93.15%	94.49%	95.74%	94.89%	94.54%	**96.73%**
SEN	99.09%	98.15%	98.82%	100%	100%	98.48%	100%	100%	100%	100%	98.75%	100%	**100%**
F1	96.21%	96.24%	96.39%	96.68%	97.04%	96.13%	96.48%	96.28%	97.04%	97.68%	96.74%	97.11%	**97.81%**
	IS_6												
ACC	100%	99.00%	99.00%	100%	100%	99.25%	99.50%	100%	100%	100%	100%	100%	**100%**
PRE	100%	98.67%	97.92%	100%	100%	99.11%	99.17%	100%	100%	100%	100%	100%	**100%**
SEN	100%	99.58%	100%	100%	100%	99.58%	100%	100%	100%	100%	100%	100%	**100%**
F1	100%	99.11%	98.90%	100%	100%	99.34%	99.57%	100%	100%	100%	100%	100%	**100%**
	IS_7												
ACC	93.85%	93.70%	93.33%	94.44%	96.15%	94.81%	95.19%	95.56%	95.38%	97.86%	96.15%	96.32%	**99.29%**
PRE	91.32%	92.26%	93.94%	92.86%	95.07%	93.46%	93.95%	93.53%	92.57%	96.78%	94.07%	97.23%	**98.89%**
SEN	98.33%	95.65%	92.62%	96.42%	98.75%	96.62%	96.41%	99.00%	100%	100%	100%	95.48%	**100%**
F1	94.42%	93.90%	92.99%	93.91%	96.61%	94.92%	94.94%	95.82%	95.85%	98.30%	96.69%	96.21%	**99.41%**
	IS_8												
ACC	97.50%	96.18%	97.06%	97.27%	95.00%	96.18%	97.06%	98.18%	95.00%	97.31%	98.89%	98.00%	**99.20%**
PRE	95.00%	94.39%	97.50%	93.50%	95.00%	94.38%	96.39%	96.00%	95.00%	96.86%	97.56%	96.33%	**99.09%**
SEN	100%	98.12%	97.20%	100%	96.00%	98.12%	98.04%	**100%**	96.00%	98.04%	**100%**	**100%**	99.33%
F1	97.09%	96.11%	97.10%	96.35%	94.87%	96.11%	96.95%	97.78%	94.87%	97.35%	98.68%	97.98%	**99.18%**
	IS_9												
ACC	100%	100%	100%	100%	100%	100%	100%	100%	100%	100%	100%	100%	**100%**
PRE	100%	100%	100%	100%	100%	100%	100%	100%	100%	100%	100%	100%	**100%**
SEN	100%	100%	100%	100%	100%	100%	100%	100%	100%	100%	100%	100%	**100%**
F1	100%	100%	100%	100%	100%	100%	100%	100%	100%	100%	100%	100%	**100%**
	IS_10												
ACC	96.64%	97.59%	96.67%	96.32%	95.36%	97.59%	97.37%	95.79%	96.07%	97.90%	97.79%	97.83%	**98.06%**
PRE	97.64%	98.14%	96.98%	96.33%	97.71%	97.87%	97.39%	96.30%	99.17%	98.61%	**99.43%**	98.18%	98.29%
SEN	95.40%	96.98%	96.30%	96.37%	92.89%	97.14%	97.43%	95.26%	92.89%	97.21%	96.16%	97.59%	**97.94%**
F1	96.50%	97.52%	96.56%	96.30%	95.07%	97.52%	97.34%	95.67%	95.80%	97.89%	97.75%	97.85%	**98.10%**
	IS_11												
ACC	96.46%	96.62%	96.88%	96.67%	96.88%	97.08%	95.94%	97.62%	96.25%	98.00%	98.13%	98.24%	**98.28%**
PRE	98.81%	98.97%	98.45%	98.57%	98.89%	99.12%	99.09%	98.57%	99.00%	98.93%	98.57%	**100%**	98.78%
SEN	94.38%	94.31%	95.14%	95.43%	95.89%	95.17%	92.67%	97.09%	93.76%	97.06%	97.33%	96.83%	**97.81%**
F1	96.50%	96.54%	96.72%	96.79%	97.25%	97.06%	95.66%	97.63%	96.07%	97.96%	97.80%	98.32%	**98.37%**
	IS_12												
ACC	100%	99.68%	100%	100%	100%	99.76%	100%	100%	100%	100%	100%	100%	**100%**
PRE	100%	99.85%	100%	100%	100%	99.85%	100%	100%	100%	100%	100%	100%	**100%**
SEN	100%	99.53%	100%	100%	100%	99.68%	100%	100%	100%	100%	100%	100%	**100%**
F1	100%	99.69%	100%	100%	100%	99.76%	100%	100%	100%	100%	100%	100%	**100%**
	IS_13												
ACC	98.75%	96.33%	98.75%	98.75%	100%	96.33%	98.75%	99.38%	99.17%	99.38%	100%	100%	**100%**
PRE	97.78%	98.36%	99.41%	98.89%	100%	97.99%	97.27%	98.89%	98.57%	99.09%	100%	100%	**100%**
SEN	100%	94.51%	98.56%	98.33%	100%	94.84%	100%	100%	100%	100%	100%	100%	**100%**
F1	98.82%	96.34%	98.95%	98.50%	100%	96.27%	98.56%	99.41%	99.23%	99.52%	100%	100%	**100%**

TABLE V
(Continued.) SUBJECT COMPARISON OF DIFFERENT METHODS ON THE ZUCH DATASET

	IS_14												
ACC	98.46%	96.79%	96.92%	98.89%	93.33%	97.50%	98.46%	98.89%	96.67%	99.09%	100%	100%	**100%**
PRE	97.89%	94.31%	94.23%	100%	88.50%	95.22%	97.50%	98.33%	93.00%	97.50%	100%	100%	**100%**
SEN	100%	99.33%	100%	98.57%	100%	100%	100%	100%	100%	100%	100%	100%	**100%**
F1	98.89%	96.64%	96.89%	99.23%	93.02%	97.46%	98.57%	99.09%	95.56%	98.57%	100%	100%	**100%**
	IS_15												
ACC	98.18%	97.35%	98.82%	98.18%	98.82%	97.35%	98.82%	98.64%	98.82%	98.89%	99.60%	99.44%	**99.62%**
PRE	98.75%	97.59%	97.89%	98.56%	**100%**	97.63%	98.39%	98.06%	100%	98.75%	**100%**	**100%**	98.89%
SEN	98.17%	97.11%	100%	98.29%	97.75%	97.05%	99.47%	99.17%	97.75%	98.89%	99.38%	99.00%	**100%**
F1	98.37%	97.34%	98.90%	98.36%	98.81%	97.28%	98.90%	98.58%	98.81%	98.75%	99.68%	99.47%	**99.41%**
	IS_16												
ACC	97.50%	96.18%	97.06%	97.27%	95.00%	96.18%	97.06%	98.18%	95.00%	97.95%	98.67%	97.78%	**99.20%**
PRE	95.00%	94.39%	97.50%	93.50%	95.00%	94.38%	96.39%	96.00%	95.00%	98.25%	97.75%	93.33%	**99.09%**
SEN	100%	98.12%	97.20%	100%	96.00%	98.12%	98.04%	97.52%	96.00%	97.58%	100%	100%	**100%**
F1	97.09%	96.11%	97.10%	96.35%	94.87%	96.11%	96.95%	97.78%	94.87%	97.87%	98.81%	95.76%	**99.18%**
	IS_17												
ACC	100%	100%	100%	100%	98.75%	99.41%	100%	100%	98.75%	100%	100%	100%	**100%**
PRE	100%	100%	100%	100%	100%	100%	100%	100%	100%	100%	100%	100%	**100%**
SEN	100%	100%	100%	100%	98.00%	98.89%	100%	100%	98.00%	100%	100%	100%	**100%**
F1	100%	100%	100%	100%	98.89%	99.41%	100%	100%	98.89%	100%	100%	100%	**100%**
	IS_18												
ACC	99.23%	97.50%	98.00%	96.15%	97.78%	98.25%	98.00%	99.23%	97.78%	99.38%	99.44%	100%	**100%**
PRE	100%	98.65%	100%	95.24%	96.33%	100%	100%	100%	96.33%	100%	100%	100%	**100%**
SEN	98.57%	96.35%	95.32%	96.90%	100%	96.46%	95.84%	98.33%	100%	98.75%	99.17%	100%	**100%**
F1	99.23%	97.43%	97.38%	96.00%	97.98%	98.16%	97.75%	99.09%	97.98%	99.33%	99.57%	100%	**100%**
	IS_19												
ACC	98.33%	97.45%	98.40%	95.29%	95.83%	97.65%	98.00%	97.06%	96.67%	99.00%	98.63%	98.75%	**99.09%**
PRE	100%	99.44%	100%	100%	100%	100%	100%	100%	100%	100%	100%	100%	**100%**
SEN	95.50%	95.33%	96.22%	91.32%	90.72%	95.12%	95.70%	95.31%	92.39%	98.18%	97.32%	96.89%	**98.29%**
F1	97.46%	97.33%	97.98%	95.17%	94.57%	97.48%	97.75%	97.50%	95.48%	99.05%	98.62%	98.35%	**99.10%**
	IS_20												
ACC	98.24%	96.76%	97.06%	95.45%	96.25%	96.76%	97.65%	96.36%	96.25%	98.80%	97.83%	98.00%	**98.87%**
PRE	**100%**	**100%**	**100%**	**100%**	**100%**	99.44%	**100%**	**100%**	**100%**	99.44%	**100%**	**100%**	99.43%
SEN	96.90%	93.62%	94.76%	90.42%	94.00%	94.15%	96.19%	91.67%	94.00%	98.07%	95.65%	95.89%	**98.21%**
F1	98.32%	96.64%	97.18%	94.48%	96.39%	96.68%	97.95%	95.14%	96.39%	98.74%	97.68%	97.80%	**98.81%**
	IS_21												
ACC	98.57%	99.05%	97.00%	94.29%	94.00%	98.57%	97.00%	94.29%	94.00%	99.48%	98.00%	99.09%	**99.82%**
PRE	97.75%	97.75%	94.90%	82.17%	89.17%	97.75%	96.33%	82.17%	89.17%	99.02%	97.57%	98.00%	**99.71%**
SEN	99.17%	100.00%	100.00%	90.00%	100.00%	99.17%	98.57%	90.00%	100.00%	100.00%	98.57%	100.00%	**100%**
F1	98.37%	98.81%	97.21%	85.46%	93.23%	98.37%	97.21%	85.46%	93.24%	99.50%	98.05%	98.89%	**99.85%**
	IS_22												
ACC	98.00%	95.81%	98.67%	95.00%	95.71%	97.42%	97.33%	96.00%	92.86%	98.08%	98.75%	99.00%	**99.00%**
PRE	96.78%	93.46%	97.89%	91.31%	82.17%	96.45%	95.35%	92.64%	80.67%	96.50%	96.67%	**98.50%**	98.23%
SEN	100%	98.82%	100%	100%	90.00%	98.89%	100%	100%	90.00%	100%	100%	100%	**100%**
F1	98.00%	95.95%	97.89%	94.90%	85.46%	97.57%	97.53%	95.79%	84.39%	98.11%	98.00%	**99.22%**	99.07%
	IS_23												
ACC	98.21%	97.91%	98.14%	97.86%	97.62%	97.79%	97.91%	98.21%	98.10%	98.75%	98.65%	98.93%	**98.95%**
PRE	98.12%	97.79%	97.26%	98.12%	96.35%	97.61%	97.26%	98.12%	97.06%	97.80%	97.44%	98.02%	**99.05%**
SEN	98.45%	98.04%	99.47%	97.62%	98.75%	98.07%	89.18%	98.45%	98.75%	**100%**	**100%**	**100%**	98.86%
F1	98.22%	97.89%	98.30%	97.75%	97.34%	97.80%	98.02%	98.22%	97.71%	98.86%	98.67%	98.93%	**98.95%**
	IS_24												
ACC	98.67%	97.94%	99.68%	99.05%	100%	98.10%	99.68%	99.52%	100%	100%	100%	100%	**100%**
PRE	99.00%	99.37%	100%	98.75%	100%	98.73%	100%	98.75%	100%	100%	100%	100%	**100%**
SEN	98.89%	96.59%	99.38%	99.17%	100%	97.45%	99.38%	100%	100%	100%	100%	100%	**100%**
F1	98.89%	97.94%	99.68%	98.90%	100%	98.07%	99.68%	99.33%	100%	100%	100%	100%	**100%**
	IS_25												
ACC	97.69%	96.54%	96.15%	96.25%	98.33%	97.69%	96.15%	97.50%	96.67%	98.28%	97.69%	98.00%	**99.00%**
PRE	98.03%	97.18%	95.83%	92.50%	98.00%	97.98%	95.83%	95.00%	96.00%	98.50%	97.98%	98.00%	**98.57%**
SEN	97.41%	96.65%	96.90%	100%	100%	97.95%	96.90%	100%	100%	97.85%	97.95%	99.09%	**100%**
F1	97.65%	96.88%	96.23%	95.66%	98.89%	97.95%	96.23%	96.67%	97.78%	98.20%	97.95%	98.41%	**99.23%**
	Average												
ACC	97.36%	97.13%	96.77%	97.11%	97.59%	97.70%	97.77%	98.01%	97.66%	97.98%	97.96%	97.81%	**98.08%**
PRE	97.19%	97.81%	96.87%	96.60%	97.24%	97.85%	97.78%	97.73%	97.27%	97.89%	97.37%	97.21%	**97.93%**
SEN	97.54%	97.03%	96.67%	97.23%	98.17%	97.55%	97.75%	98.16%	98.11%	98.04%	98.40%	98.44%	**98.46%**
F1	97.36%	97.42%	96.77%	97.91%	98.00%	97.70%	97.77%	98.03%	97.69%	97.98%	97.97%	97.82%	**98.09%**

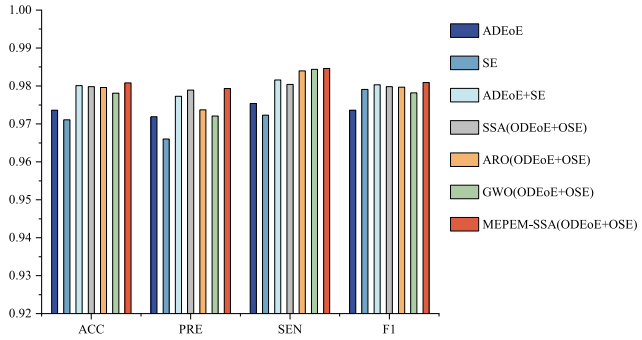

Fig. 6. Average classification results under different methods on the ZUCH dataset.

TABLE VI
CHANGES IN CLASSIFICATION PERFORMANCE OF ADEOE DUE TO DIFFERENT t'S WHEN $j = 20$ ON THE CHB-MIT DATASET

	Classifier	t=1(%)	t=2(%)	t=3(%)	t=4(%)	t=5(%)	t=6(%)	t=7(%)	t=8(%)
ACC	RF	95.31	97.06	96.62	97.16	97.30	97.50	96.64	96.67
	KNN	97.20	98.65	98.35	98.42	98.24	97.73	97.76	97.42
	SVM	96.52	97.58	97.16	97.55	96.98	97.66	97.57	97.31
PRE	RF	95.79	96.96	95.64	96.40	96.78	96.60	96.01	95.50
	KNN	97.96	99.11	99.00	99.02	98.89	98.96	98.72	98.56
	SVM	96.76	97.66	96.74	97.36	96.74	97.33	97.05	96.37
SEN	RF	93.94	96.48	96.45	96.93	96.63	96.95	95.03	95.14
	KNN	95.92	97.86	97.17	97.63	96.82	95.19	95.04	94.33
	SVM	95.65	96.93	96.54	96.77	95.90	96.60	96.39	96.15
F1	RF	94.84	96.71	96.04	96.63	96.69	96.76	95.45	95.27
	KNN	96.92	98.48	98.07	98.35	97.83	97.02	96.76	96.35
	SVM	96.20	97.28	96.63	97.04	96.30	96.95	96.68	96.24

TABLE VII
CHANGES IN CLASSIFICATION PERFORMANCE OF ADEOE DUE TO DIFFERENT j'S WHEN $t = 2$ ON THE CHB-MIT DATASET

	Classifier	j=5(%)	j=10(%)	j=15(%)	j=20(%)	j=25(%)	j=30(%)
ACC	RF	94.55	96.43	96.60	97.06	95.94	96.22
	KNN	96.53	98.18	98.44	98.65	98.28	98.32
	SVM	95.97	97.20	97.37	97.58	96.69	96.99
PRE	RF	92.82	95.13	95.96	96.96	96.28	96.50
	KNN	96.33	98.53	98.79	99.11	98.58	98.84
	SVM	95.14	96.83	97.03	97.66	97.09	97.40
SEN	RF	95.14	96.98	96.47	96.48	94.59	94.99
	KNN	95.88	97.39	97.70	97.86	97.55	97.39
	SVM	95.88	96.91	97.08	96.93	95.46	95.82
F1	RF	93.96	96.04	96.21	96.71	95.42	95.73
	KNN	96.10	97.95	98.24	98.48	98.06	98.11
	SVM	95.50	96.87	97.05	97.28	96.26	96.60

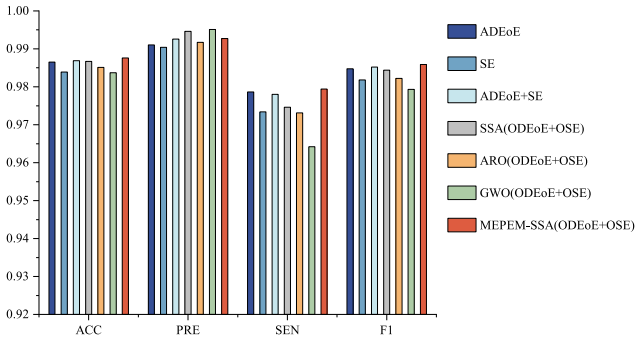

Fig. 7. Average classification results under different methods on the CHB-MIT dataset.

As shown in Fig. 6, MEPEM-SSA combined with ODEoE + OSE fusion feature outperforms the other centralized models in all performance metrics. For ADEoE, MEPEM-SSA combined with ODEoE + OSE fusion feature improves ACC, PRE, SEN, and $F1$ by 0.72%, 0.74%, 0.92%, and 0.7%, respectively. Comparing with SE, MEPEM-SSA combined with ODEoE + OSE fusion feature improves ACC, PRE, SEN, and $F1$ by 0.97%, 1.33%, 1.23%, and 0.18%, respectively. Comparing parameter optimization with SSA, the method of MEPEM-SSA combined with ODEoE + OSE fusion feature improves ACC, PRE, SEN, and $F1$ by 0.1%, 0.4%, 0.42%, and 0.11%, respectively. Comparing with parameter optimization with ARO, the method of MEPEM-SSA combined with ODEoE + OSE fusion feature improves ACC, PRE, SEN, and $F1$ by 0.12%, 0.56%, 0.06%, and 0.12%, respectively. Comparing with parameter optimization with GWO, the method of MEPEM-SSA combined with ODEoE + OSE fusion feature improves ACC, PRE, SEN, and $F1$ by 0.27%, 0.72%, 0.02%, and 0.27%, respectively.

C. CHB-MIT Dataset Result

The results of ADEoE parameters with different classifiers on the CHB-MIT dataset will be analyzed in the same way. In Table VI, the classification performance differences of RF, KNN, and SVM classifiers with different t values when $j = 20$ are compared. In Table VII, the classification performance of different classifiers with different j values when $t = 2$ is compared. Combining the analysis of these two parameters, KNN performs the best results when $t = 2$ and $j = 20$, and the ACC reaches 98.65%. Thus, we select these optimal parameters of ADEoE to calculate the results in the subsequent experiments.

Table VIII shows the classification performance of seizure detection using different feature values, including SE, ADEoE + SE fusion features, and ODEoE + OSE fusion features. The experiment separately calculates the classification performance of SE and ADEoE + SE fusion features when selecting different t values on KNN. It can be seen that the classification results will fluctuate to varying degrees with the change of t. The classification performance of ADEoE is partially higher than SE, and the overall performance of ADEoE + SE fusion features is better than SE. Then, different optimization algorithms are used to optimize the ODEoE + OSE fusion feature, including SSA, ARO, GWO, and MEPEM-SSA. The results indicate that the method of MEPEM-SSA combined with ODEoE + OSE fusion feature yields the best results of classification, with average ACC, SEN, and $F1$ metrics of 98.76%, 97.94%, and 98.59%, respectively. Fig. 7 shows the classification performance of several methods. For SE, MEPEM-SSA combined with ODEoE + OSE fusion feature improves ACC, PRE, SEN, and $F1$ by 0.37%, 0.23%, 0.60%, and 0.41%, respectively. Compared

TABLE VIII
COMPARISON OF DIFFERENT METHODS ON THE CHB-MIT DATASET

	SE				SE+ADEoE				OSE+ODEoE			
	t=2	t=4	t=6	t=8	t=2	t=4	t=6	t=8	SSA	ARO	GWO	MEPEM-SSA
ACC	98.39%	98.38%	98.05%	96.56%	98.69%	98.63%	98.05%	97.20%	98.67%	98.51%	98.37%	**98.76%**
PRE	99.04%	99.65%	99.58%	98.16%	99.26%	99.52%	**99.57%**	98.51%	99.46%	99.17%	99.51%	99.27%
SEN	97.34%	96.49%	95.51%	92.49%	97.80%	97.19%	95.43%	93.82%	97.46%	97.31%	96.42%	**97.94%**
F1	98.18%	98.03%	97.45%	95.19%	98.52%	98.33%	97.43%	96.06%	98.44%	98.22%	97.93%	**98.59%**

TABLE IX
CHANGES IN CLASSIFICATION PERFORMANCE OF ADEOE DUE TO DIFFERENT t WHEN $j = 20$ ON THE SIENA SCALP EEG DATASET

	Classifier	t=1(%)	t=2(%)	t=3(%)	t=4(%)	t=5(%)	t=6(%)	t=7(%)	t=8(%)
ACC	RF	94.58	93.26	93.06	92.93	93.59	93.60	94.53	95.09
	KNN	97.38	96.99	95.80	95.60	94.24	96.27	94.84	96.18
	SVM	96.26	95.82	94.97	94.83	94.89	95.07	94.69	93.82
PRE	RF	91.83	90.48	91.46	91.32	91.69	92.06	91.98	93.73
	KNN	96.51	96.46	94.82	95.62	92.91	96.42	94.65	95.42
	SVM	95.28	94.63	94.05	94.27	93.12	94.57	92.63	92.28
SEN	RF	97.31	95.82	94.04	93.81	94.25	93.69	96.17	94.94
	KNN	98.03	97.17	96.33	95.00	94.12	95.12	93.89	95.72
	SVM	97.01	96.72	95.36	94.75	95.68	94.30	96.01	93.84
F1	RF	94.48	93.05	92.69	92.39	92.90	92.85	93.97	94.28
	KNN	97.26	96.81	95.54	95.22	93.42	95.70	94.18	95.48
	SVM	96.13	95.64	94.68	94.41	94.34	94.39	94.15	93.00

TABLE X
CHANGES IN CLASSIFICATION PERFORMANCE OF ADEOE DUE TO DIFFERENT j WHEN $t = 6$ ON THE SIENA SCALP EEG DATASET

	Classifier	j=5(%)	j=10(%)	j=15(%)	j=20(%)	j=25(%)	j=30(%)
ACC	RF	90.40	92.13	92.27	93.60	92.40	94.53
	KNN	91.47	95.60	94.66	96.27	94.80	95.60
	SVM	92.13	94.53	94.27	95.07	95.07	95.33
PRE	RF	87.48	90.34	89.82	92.06	90.91	93.77
	KNN	95.39	95.50	94.57	96.42	94.69	95.33
	SVM	90.44	93.45	92.10	94.57	93.52	93.35
SEN	RF	91.68	92.22	93.13	93.69	92.21	94.11
	KNN	85.17	94.72	93.41	95.12	93.77	94.95
	SVM	92.27	94.28	95.15	94.30	95.47	96.42
F1	RF	89.45	91.22	91.39	92.85	91.52	93.89
	KNN	89.86	95.07	93.94	95.70	94.18	95.09
	SVM	91.27	93.80	93.58	94.39	94.46	94.83

to ADEoE + SE fusion feature, MEPEM-SSA combined with ODEoE + OSE fusion feature improves ACC, SEN, and $F1$ by 0.07%, 0.14%, and 0.07%, respectively. Compared to parameter optimization with SSA, the method of MEPEM-SSA combined with ODEoE + OSE fusion feature improves ACC, SEN, and $F1$ by 0.09%, 0.48%, and 0.15%, respectively. Compared to parameter optimization with ARO, the method of MEPEM-SSA combined with ODEoE + OSE fusion feature improves ACC, PRE, SEN, and $F1$ by 0.25%, 0.10%, 0.63%, and 0.37%, respectively. Compared to parameter optimization with GWO, the method of MEPEM-SSA combined with ODEoE + OSE fusion feature improves ACC, SEN, and $F1$ by 0.39%, 1.52%, and 0.66%, respectively.

D. Siena Scalp EEG Dataset Result

Similarly, the results of ADEoE parameters and classifiers on the Siena Scalp EEG dataset are discussed as follows. In Table IX, the classification performance differences of RF, KNN, and SVM classifiers with different t values when $j = 20$ are compared. Table X shows the classification performance of different classifiers with different j values when $t = 6$. Combining the analysis of these two tables, KNN performs the best results when $t = 6$ and $j = 20$; the ACC reaches 96.27%. In the subsequent experiments, the optimal parameters of ADEoE and KNN classifier are selected to continue our research.

Table XI shows the classification performance using different feature values on the Siena dataset, including SE, ADEoE + SE fusion features, and ODEoE + OSE fusion features optimized through different optimization algorithms. First, the classification performance of SE and ADEoE + SE fusion features is calculated when selecting different t values. Comparing Tables IX and X, it can be seen that the classification performance of ADEoE is higher than SE, and the overall performance of ADEoE + SE fusion features is better than SE. Then, different optimization algorithms are used to optimize the ODEoE + OSE fusion feature, including SSA, ARO, GWO, and MEPEM-SSA. The results show that the method combining MEPEM-SSA with ODEoE + OSE fusion features produced the best classification results on average ACC, PRE, and $F1$ indicators, with scores of 98.33%, 98.04%, and 98.20%, respectively. Fig. 8 shows the classification performance of several methods. For SE,

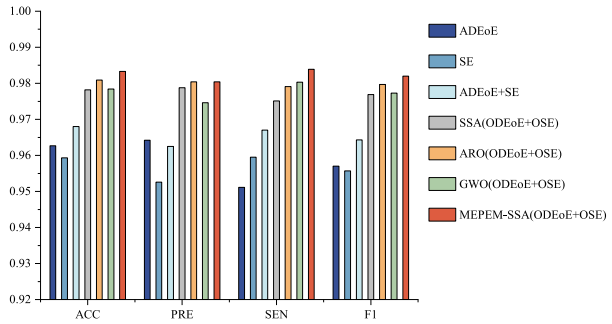

Fig. 8. Average classification results under different methods on the Siena Scalp EEG dataset.

TABLE XI
COMPARISON OF DIFFERENT METHODS ON THE SIENA SCALP EEG DATASET

	SE				ADEoE+SE				ODEoE+OSE			
	t=2	t=4	t=6	t=8	t=2	t=4	t=6	t=8	SSA	ARO	GWO	MEPEM-SSA
ACC	97.60%	97.59%	95.93%	97.09%	97.82%	97.33%	96.80%	97.45%	97.82%	98.09%	97.84%	**98.33%**
PRE	96.87%	97.33%	95.26%	95.34%	97.88%	96.60%	96.25%	95.42%	97.88%	98.04%	97.46%	**98.04%**
SEN	97.28%	97.37%	95.95%	98.29%	97.51%	97.65%	96.70%	**98.61%**	97.51%	97.91%	98.03%	98.39%
F1	97.57%	97.32%	95.57%	96.74%	97.69%	97.08%	96.43%	96.95%	97.69%	97.97%	97.73%	**98.20%**

TABLE XII
COMPARISON OF PERFORMANCE ON EXISTING SEIZURE DETECTION METHODS

Author	Methodology	Dataset	ACC	PRE	SEN	F1
Cimr D et al. [29]	Computer-aided diagnosis	CHB-MIT	96.99%	96.89%	97.06%	-
Chakrabarti S et al. [30]	DWT	CHB-MIT	95.30%	-	97.20%	-
Xiong Y et al. [31]	Fusion of spatio-temporal network	CHB-MIT	97.83%	97.56%	98.24%	97.89%
Cao J et al. [32]	SCNNs+AWF	CHB-MIT	**99.62%**	-	97.17%	93.90%
Gao Y et al. [33]	EESC	CHB-MIT	92.60%	-	92.60%	-
Peng H et al. [34]	DLWH	CHB-MIT	95.06%	-	95.38%	-
Zhang W et al. [19]	ARO based MLNDP	ZUCH	97.18%	97.03%	97.43%	97.16%
Our work	ODEoE+OSE+MEPEM-SSA	Siena scalp EEG	98.33%	98.04%	98.39%	98.20%
Our work	ODEoE+OSE+MEPEM-SSA	CHB-MIT	98.76%	**99.27%**	97.94%	**98.59%**
Our work	ODEoE+OSE+MEPEM-SSA	ZUCH	98.08%	97.93%	**98.46%**	98.09%

MEPEM-SSA combined with ODEoE + OSE fusion feature improves ACC, PRE, SEN, and $F1$ by 2.4%, 2.78%, 2.44%, and 2.63%, respectively. Compared to ADEoE + SE fusion feature, MEPEM-SSA combined with ODEoE + OSE fusion feature improves ACC, PRE, and $F1$ by 1.53%, 1.79%, and 1.77%, respectively. Compared to parameter optimization with SSA, the method of MEPEM-SSA combined with ODEoE + OSE fusion feature improves ACC, PRE, SEN, and $F1$ by 0.51%, 0.16%, 0.88%, and 0.51%, respectively. Compared to parameter optimization with ARO, the method of MEPEM-SSA combined with ODEoE + OSE fusion feature improves ACC, SEN, and $F1$ by 0.24%, 0.48%, and 0.23%, respectively. Compared to parameter optimization with GWO, the method of MEPEM-SSA combined with ODEoE + OSE fusion feature improves ACC, PRE, SEN, and $F1$ by 0.49%, 0.58%, 0.36%, and 0.47%, respectively.

IV. DISCUSSION

In this article, we first use EEG sensors to extract EEG signals, then perform WPT on the preprocessed EEG signals, and then use ODEoE for precise detection of seizures. Unlike the common EoE, ODEoE calculates both the length of the epoch and the number of subepochs in one epoch as parameters. In the experiment, different classification performances can be achieved by simultaneously changing these two important parameters. Then, use MEPEM-SSA to perform parameter optimization calculations on the ODEoE + OSE fusion feature. MEPEM-SSA is an SSA algorithm that combines tent mapping and random walk strategy, which is believed to reduce the impact of uneven initial population distribution and the tendency to fall into local optima. In the feature extraction section, three types of feature values are used to compare the performance of classification. Finally, the feature values are fed into RF, KNN, and SVM classifiers for seizure detection. According to the experiment, the fusion feature values of OSE and ODEoE have the best classification performance.

This article only studies the classification of the data extracted from EEG sensors, without considering whether the data extracted from different sensors will affect the classification results. In future work, we can analyze and study the fusion of multiple sensor data, which may further improve the performance of ODEoE. In addition, this article considers the binary situation of seizures and nonseizures and has not yet studied the multiclassification of epileptic seizures. In the next step of research, we can further achieve automatic multiclassification detection of epilepsy using ODEoE. In Table XII, we compare existing seizure detection methods with our methods in terms of research methods, dataset, and detection results. Different datasets use EEG sensors to extract data. Cimr et al. [32] proposed a computer-aided diagnosis-based seizure detection algorithm. The ACC, PRE, and SEN evaluated on the CHB-MIT dataset are 96.99%, 96.89%, and 97.06%, respectively. Chakrabarti et al. [33] combined DWT and artificial neural network to evaluate CHB-MIT. The ACC and SEN achieve 95.30% and 97.20%, respectively. Xiong et al. [34] proposed a seizure detection algorithm based on the fusion of a spatiotemporal network constructed with a dispersion index. The ACC, PRE, SEN, and F1 on CHB-MIT are 97.83%, 97.56%, 98.24%, and 97.89%, respectively. Cao et al. [35] combined stacked convolutional neural networks (SCNNs) and adaptive feature weighting fusion (AWF) to evaluate CHB-MIT. The ACC, SEN, and $F1$ achieve 99.62%, 97.17%, and 93.90%, respectively. A new deep learning-based classification methodology, namely, epileptic EEG signal classification (EESC), was proposed by Gao et al. [36]. The ACC and SEN evaluated on the CHB-MIT dataset are 92.60% and 92.60%, respectively. Peng et al. [37] proposed a seizure detection algorithm based on dictionary learning with homotopy (DLWH). The ACC

and SEN evaluated on the CHB-MIT dataset are 95.06% and 95.38%, respectively. Zhang et al. [22] used ARO to select the optimal MLNDP for seizure detection. The ACC, PRE, SEN, and $F1$ on the ZUCH dataset are 97.18%, 97.03%, 97.43%, and 97.16%, respectively. Cimr et al. [32], Chakrabarti et al. [33], Xiong et al. [34], Cao et al. [35], Gao et al. [36], and Peng et al. [37] all used the CHB-MIT dataset for seizure detection experiments. Among them, ACC in [35] reaches the maximum value, which is 99.62%, and ACC in [36] is the smallest at 92.60%. PRE, SEN, and $F1$ in [34] reach the maximum values, which are 97.56%, 98.24%, and 97.89%, respectively. Compared with all methods, the ODEoE + OSE fusion feature combined with the MEPEM-SSA method on the CHB-MIT dataset achieves the maximum PRE and $F1$ performance with a result of 99.27% and 98.59%. The results on the ZUCH dataset achieve the maximum SEN at 98.46%.

V. Conclusion

This article focuses on seizure detection of West syndrome from EEG sensor data. To achieve this goal, this article proposes an ADEoE with adjustable parameters based on EoE and then combines MEPEM-SSA to optimize the ODEoE + OSE fusion features. EoE extracts the information and the degree of information change hidden in the time series by calculating SE twice on the time series using a multiscale method. First, unlike traditional EoE methods, ADEoE has two parameters in the calculation process: epoch length and the number of subepochs in one epoch, and changing these two parameters can result in significant differences in ADEoE values. Next, the obtained ADEoE and SE will be fused into features, and intelligent algorithms will be used to find the optimal fusion feature of ODEoE and OSE. The optimal parameter selection depends on MEPEM-SSA. This utilizes tent chaotic mapping and random walk strategy to improve the search and optimization ability of the algorithm.

The method is evaluated through epileptic seizure detection experiments using three datasets obtained from EEG sensors. This article uses the CHB-MIT and Siena Scalp EEG datasets together with the ZUCH dataset for training data, aiming to demonstrate the generality of the method. The conclusion indicates that the proposed model performs well on all three datasets, further demonstrating the universality of this method. On the ZUCH dataset, ACC, PRE, SEN, and $F1$ reach 98.08%, 97.93%, 98.46%, and 98.09%, respectively. On the CHB-MIT dataset, ACC, PRE, SEN, and $F1$ of the method proposed reach 98.76%, 99.27%, 97.94%, and 98.59%, respectively. On the Siena Scalp EEG dataset, ACC, PRE, SEN, and $F1$ of the method proposed in this article reach 98.33%, 98.04%, 98.39%, and 98.20%, respectively.

The experimental results show that the performance of ODEoE + OSE fusion features is better than that of ADEoE, SE, and ADEoE + SE fusion features. The use of MEPEM-SSA for parameter optimization behaves better than general optimizers. Thus, the combination of MEPEM-SSA and ODEoE + OSE fusion features is an effective feature extraction technique for epileptic seizure detection. This method combined with EEG sensors shows excellent classification results on different datasets. It has a good effect on the detection of epileptic seizures and has a significant impact on the medical diagnosis of epilepsy. In the future, we will further explore the performance of this method on multimodal signals combining EEG and EMG and investigate its impact on epilepsy classification under different biological signals.

Acknowledgment

Yue Bi and Yi Lin are with the School of Communication Engineering, Hangzhou Dianzi University, Hangzhou 310018, China (e-mail: bbiyuez@163.com; lizdeemail1230@163.com).

Duanpo Wu is with the School of Communication Engineering and the Artificial Intelligence Institute, Hangzhou Dianzi University, Hangzhou, Zhejiang 310018, China (e-mail: wuduanpo@hdu.edu.cn).

Zhaoyang Xu is with the Department of Paediatrics, University of Cambridge, Hangzhou 310018, China (e-mail: zx265@cam.ac.uk).

Pierre-Paul Vidal is with the Machine Learning and I-health International Cooperation Base of Zhejiang Province, Hangzhou Dianzi University, Hangzhou 310018, China, also with the Centre Borelli, CNRS, SSA, INSERM, Université Paris Cité, 75006 Paris, France, also with ENS Paris Saclay, Université Paris Saclay, 75006 Paris, France, and also with the Plateforme d'Etude de la Sensorimotricité, INSERM US36, CNRS UAR2009, Université de Paris, 75006 Paris, France (e-mail: pierre-paul.vidal@u-paris.fr).

Danping Wang is with the Machine Learning and I-health International Cooperation Base of Zhejiang Province, Hangzhou Dianzi University, Hangzhou 310018, China, and also with the Plateforme d'Etude de la Sensorimotricité (PES), BioMedTech Faciliti, Université Paris Cité, 75270 Paris, France (e-mail: danping.wang@u-paris.fr).

Tiejia Jiang is with the Children's Hospital, Zhejiang University School of Medicine, Hangzhou 310052, China (e-mail: jiangyouze@zju.edu.cn).

Jiuwen Cao is with the Machine Learning and I-health International Cooperation Base of Zhejiang Province and the Artificial Intelligence Institute, Hangzhou Dianzi University, Hangzhou, Zhejiang 310018, China, (e-mail: jwcao@hdu.edu.cn).

Yuansheng Xu is with the Affiliated Hangzhou First People's Hospital, Zhejiang University School of Medicine, Hangzhou 310018, China (e-mail: xys0912@163.com).

References

[1] S. Chen et al., "Deterministic learning-based WEST syndrome analysis and seizure detection on ECG," *IEEE Trans. Circuits Syst. II, Exp. Briefs*, vol. 69, no. 11, pp. 4603–4607, Nov. 2022.

[2] X. Cui, J. Cao, D. Hu, T. Wang, T. Jiang, and F. Gao, "Regional scalp EEGs analysis and classification on typical childhood epilepsy syndromes," *IEEE Trans. Cogn. Develop. Syst.*, vol. 15, no. 2, pp. 662–674, Jun. 2022.

[3] P. Pavone, P. Striano, R. Falsaperla, L. Pavone, and M. Ruggieri, "Infantile spasms syndrome, west syndrome and related phenotypes: What we know in 2013," *Brain Develop.*, vol. 36, no. 9, pp. 739–751, Oct. 2014.

[4] M. Sharma, A. A. Bhurane, and U. R. Acharya, "MMSFL-OWFB: A novel class of orthogonal wavelet filters for epileptic seizure detection," *Knowl.-Based Syst.*, vol. 160, pp. 265–277, Nov. 2018.

[5] U. R. Acharya, Y. Hagiwara, and H. Adeli, "Automated seizure prediction," *Epilepsy Behav.*, vol. 88, pp. 251–261, Nov. 2018.

[6] J. Wanigasinghe, C. Arambepola, S. S. Ranganathan, K. Jayasundara, A. Weerasinghe, and P. Wickramarachchi, "Epilepsy outcome at four years in a randomized clinical trial comparing oral prednisolone and intramuscular ACTH in west syndrome," *Pediatric Neurol.*, vol. 119, pp. 22–26, Jun. 2021.

[7] O. S. Lih et al., "EpilepsyNet: Novel automated detection of epilepsy using transformer model with EEG signals from 121 patient population," *Comput. Biol. Med.*, vol. 164, Sep. 2023, Art. no. 107312.

[8] I. Tasci et al., "Epilepsy detection in 121 patient populations using hypercube pattern from EEG signals," *Inf. Fusion*, vol. 96, pp. 252–268, Aug. 2023.

[9] A. Li et al., "Multiview transfer representation learning with TSK fuzzy system for EEG epilepsy detection," *IEEE Trans. Fuzzy Syst.*, vol. 32, no. 1, pp. 38–52, Jan. 2024.

[10] A. Russo and G. Gobbi, "A reflection on the role of genetics in the concept of 'epileptic encephalopathy' as emerged from the most recent ILEA classification of epilepsy," *Italian J. Pediatrics*, vol. 46, no. 1, pp. 1–4, 2020.

[11] M. Anita and A. M. Kowshalya, "Automatic epileptic seizure detection using MSA-DCNN and LSTM techniques with EEG signals," *Expert Syst. Appl.*, vol. 238, Mar. 2024, Art. no. 121727.
[12] T. Zhang, Y. Fu, and J. Zhang, "Deep guided attention network for joint denoising and demosaicing in real image," *Chin. J. Electron.*, vol. 33, no. 1, pp. 303–312, Jan. 2024.
[13] Z. Li, P. Wang, and Z. Wang, "FlowGANAnomaly: Flow-based anomaly network intrusion detection with adversarial learning," *Chin. J. Electron.*, vol. 33, no. 1, pp. 58–71, Jan. 2024.
[14] Y. Sinai, "Kolmogorov–Sinai entropy," *Scholarpedia*, vol. 4, no. 3, p. 2034, 2009.
[15] P. Grassberger and I. Procaccia, "Estimation of the Kolmogorov entropy from a chaotic signal," *Phys. Rev. A, Gen. Phys.*, vol. 28, no. 4, pp. 2591–2593, Oct. 1983.
[16] S. M. Pincus, "Approximate entropy as a measure of system complexity," *Proc. Nat. Acad. Sci. USA*, vol. 88, no. 6, pp. 2297–2301, 1991.
[17] M. Costa, A. L. Goldberger, and C.-K. Peng, "Multiscale entropy analysis of complex physiologic time series," *Phys. Rev. Lett.*, vol. 89, no. 6, Jul. 2002, Art. no. 068102.
[18] C. Hsu, S.-Y. Wei, H.-P. Huang, L. Hsu, S. Chi, and C.-K. Peng, "Entropy of entropy: Measurement of dynamical complexity for biological systems," *Entropy*, vol. 19, no. 10, p. 550, Oct. 2017.
[19] H. Cui, L. Zhou, Y. Li, and B. Kang, "Belief entropy-of-entropy and its application in the cardiac interbeat interval time series analysis," *Chaos, Solitons Fractals*, vol. 155, Feb. 2022, Art. no. 111736.
[20] E. Yildirim, Y. Kaya, and F. Kiliç, "A channel selection method for emotion recognition from EEG based on swarm-intelligence algorithms," *IEEE Access*, vol. 9, pp. 109889–109902, 2021.
[21] Z. Lian, L. Duan, Y. Qiao, J. Chen, J. Miao, and M. Li, "The improved ELM algorithms optimized by bionic WOA for EEG classification of brain computer interface," *IEEE Access*, vol. 9, pp. 67405–67416, 2021.
[22] W. Zhang, D. Wu, J. Cao, L. Jiang, and T. Jiang, "Multibit local neighborhood difference pattern optimization for seizure detection of west syndrome EEG signals," *IEEE Sensors J.*, vol. 23, no. 19, pp. 22693–22703, Oct. 2023.
[23] I. Attiya, M. A. Elaziz, L. Abualigah, T. N. Nguyen, and A. A. A. El-Latif, "An improved hybrid swarm intelligence for scheduling IoT application tasks in the cloud," *IEEE Trans. Ind. Informat.*, vol. 18, no. 9, pp. 6264–6272, Sep. 2022.
[24] J. Xue and B. Shen, "A novel swarm intelligence optimization approach: Sparrow search algorithm," *Syst. Sci. Control Eng.*, vol. 8, no. 1, pp. 22–34, Jan. 2020.
[25] J. Yuan et al., "DMPPT control of photovoltaic microgrid based on improved sparrow search algorithm," *IEEE Access*, vol. 9, pp. 16623–16629, 2021.
[26] B. Gao, W. Shen, H. Guan, L. Zheng, and W. Zhang, "Research on multistrategy improved evolutionary sparrow search algorithm and its application," *IEEE Access*, vol. 10, pp. 62520–62534, 2022.
[27] (2022). *CHB-Mit Scalp EEG Database (Version 1.0.0)*. [Online]. Available: https://www.physionet.org/content/chbmit/1.0.0/
[28] A. H. Shoeb, "Application of machine learning to epileptic seizure onset detection and treatment," Massachusetts Inst. Technol., Cambridge, MA, USA, Tech. Rep., 2009.
[29] P. Detti. (2022). *Siena Scalp EEG Database (Version 1.0.0)*. PhysioNet. [Online]. Available: https://www.physionet.org/content/siena-scalp-eeg/1.0.0/
[30] P. Detti, G. Vatti, and G. Z. M. de Lara, "EEG synchronization analysis for seizure prediction: A study on data of noninvasive recordings," *Processes*, vol. 8, no. 7, p. 846, Jul. 2020.
[31] M. Song et al., "Modified Harris hawks optimization algorithm with exploration factor and random walk strategy," *Comput. Intell. Neurosci.*, vol. 2022, pp. 1–23, Apr. 2022.
[32] D. Cimr, H. Fujita, H. Tomaskova, R. Cimler, and A. Selamat, "Automatic seizure detection by convolutional neural networks with computational complexity analysis," *Comput. Methods Programs Biomed.*, vol. 229, Feb. 2023, Art. no. 107277.
[33] S. Chakrabarti, A. Swetapadma, A. Ranjan, and P. K. Pattnaik, "Time domain implementation of pediatric epileptic seizure detection system for enhancing the performance of detection and easy monitoring of pediatric patients," *Biomed. Signal Process. Control*, vol. 59, May 2020, Art. no. 101930.
[34] Y. Xiong et al., "Seizure detection algorithm based on fusion of spatio-temporal network constructed with dispersion index," *Biomed. Signal Process. Control*, vol. 79, Jan. 2023, Art. no. 104155.
[35] J. Cao, J. Zhu, W. Hu, and A. Kummert, "Epileptic signal classification with deep EEG features by stacked CNNs," *IEEE Trans. Cogn. Develop. Syst.*, vol. 12, no. 4, pp. 709–722, Dec. 2020.
[36] Y. Gao, B. Gao, Q. Chen, J. Liu, and Y. Zhang, "Deep convolutional neural network-based epileptic electroencephalogram (EEG) signal classification," *Frontiers Neurol.*, vol. 11, p. 375, May 2020.
[37] H. Peng et al., "A novel automatic classification detection for epileptic seizure based on dictionary learning and sparse representation," *Neurocomputing*, vol. 424, pp. 179–192, Feb. 2021.

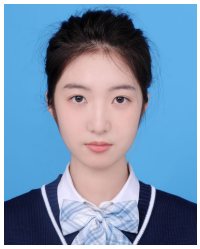

Yue Bi is currently pursuing the master's degree with Hangzhou Dianzi University, Hangzhou, China.

Her research interests include signal processing and machine learning applications in the field of epileptic seizure detection.

Duanpo Wu received the B.S. degree from the College of Electronics and Information, Hangzhou Dianzi University, Hangzhou, China, in 2009, and the Ph.D. degree from the College of Information Science and Electronic Engineering, Zhejiang University, Hangzhou, China, in 2014.

Since 2022, he has been an Associate Professor with Hangzhou Dianzi University. His research interests include intelligent signal processing, biological data analysis, and machine learning.

Zhaoyang Xu received the Ph.D. degree from the School of Electronic Engineering and Computer Science, Queen Mary University of London, London, U.K., in 2019.

Since then, he has been working as a Research Associate with the School of Clinical Medicine, Cambridge University, Cambridge, U.K. His research interests include neural science, computational biology, high-throughput biomedical image/data analysis, and artificial intelligence.

Pierre-Paul Vidal was a Principal Researcher and the Laboratory Director at the National Center for Scientific Research (CNRS), Grenoble, France, the Director of the Cognition and Behavior Group Laboratory of the French National Center for Scientific Research, the Director of the Biomedical Promotion Expert Committee of the French National Center for Scientific Research, a member of the French National Medical Research Council, the Chairperson of the Scientific Committee of the French Medical Innovation Technology Center, and a member of the Five Scientific Committees of Paris.

Danping Wang received the Engineering and M.Sc. degrees from Northeast Institute of Heavy Machinery, Qiqihaer, China, in 1982 and 1988, respectively, and the Ph.D. degree from Université de Technologie de Compiègne, Compiègne, France, in 1999.

Since 2006, she has been a Research Engineer at Université Paris Cité, France. Her research focuses on human behavior in neuroscience and biomechanics.

Yi Lin is now pursuing the B.S. degree with the School of Communication Engineering, Hangzhou Dianzi University, Hangzhou, China.

Her main research direction is signal processing and machine learning applications in seizure prediction and detection.

Tiejia Jiang received the B.S. degree from the Department of Clinical Medicine, Wenzhou Medical University, Wenzhou, China, in 2008, and the M.S. degree in pediatrics from Zhejiang University, Hangzhou, China, in 2017.

He is currently the Deputy Chief Physician with the Children's Hospital affiliated with Medical College, Zhejiang University. He is mainly engaged in electrophysiological signal analysis and research of various children's neurological diseases.

Jiuwen Cao (Senior Member, IEEE) received the B.Sc. and M.Sc. degrees from the School of Applied Mathematics, University of Electronic Science and Technology of China, Chengdu, China, in 2005 and 2008, respectively, and the Ph.D. degree from the School of Electrical and Electronic Engineering, Nanyang Technological University (NTU), Singapore, in 2013.

From 2012 to 2013, he was a Research Fellow with NTU. He is a Full Professor and the Vice Dean of the School of Automation, Hangzhou Dianzi University, Hangzhou, China. His main research interests include machine learning, neural networks, and intelligent signal processing.

Dr. Cao is an Associate Editor of IEEE TRANSACTIONS ON CIRCUITS AND SYSTEMS—PART I: REGULAR PAPER, *Journal of the Franklin Institute*, *Multidimensional Systems and Signal Processing*, *Memetic Computing*, and *Military Medical Research*.

Yuansheng Xu received the B.S. degree from the School of Medicine, Wuhan University, Wuhan, China, in 2001, the M.D. degree from the School of Medicine, Zhejiang University, Hangzhou, China, in 2007, and the Ph.D. degree from Nanjing Medical University, Nanjing, China, in 2018.

His research interests include emergency medicine and medical signal detection and processing.